

**Atomic dynamics in Zr-(Co,Ni)-Al metallic glass-forming liquids**C. C. Yuan,<sup>1,\*</sup> F. Yang,<sup>1</sup> F. Kargl,<sup>1</sup> D. Holland-Moritz,<sup>1</sup> G. G. Simeoni,<sup>2</sup> and A. Meyer<sup>1</sup><sup>1</sup>*Institut für Materialphysik im Weltraum, Deutsches Zentrum für Luft- und Raumfahrt (DLR), 51170 Köln, Germany*<sup>2</sup>*Heinz Maier-Leibnitz Zentrum (MLZ) and Physics Department, Technische Universität München, Lichtenbergstrasse 1, 85748 Garching, Germany*

(Received 14 March 2015; revised manuscript received 25 May 2015; published 11 June 2015)

The microscopic transport and the macroscopic flow behavior of Zr-(Co,Ni)-Al melts are systemically investigated using containerless processing techniques. A remarkable decrease of the Co, Ni self-diffusion coefficient and increase of the melt viscosity upon alloying Al, are observed. In contrast to many other metallic glass-forming liquids, the average packing fraction of the melt derived from the measured macroscopic density decreases. Our study indicates that chemical interactions of Al with transition metal atoms play an important role in slowing down liquid dynamics of metal melts, which also contribute to their improved glass-forming ability.

DOI: [10.1103/PhysRevB.91.214203](https://doi.org/10.1103/PhysRevB.91.214203)

PACS number(s): 66.10.cg, 66.20.-d, 71.23.-k

Metallic glass-forming (MGF) melts, without directional bonding between atoms, are generally considered as a model system close to the assumption of the hard-sphere (HS) model [1]. Compared with simple metallic melts, they exhibit considerably higher packing fraction (around 0.5) [2–4]. According to mode coupling theory (MCT), their dynamics slowing down upon approaching the glass transition is due to the localization of atoms by their neighbours, and eventually freezes in at the critical temperature  $T_c$  [5]. Close to  $T_c$ , the liquid dynamics, like melt viscosity, scales with asymptotic scaling laws [5]:

$$\eta \propto [(T - T_c)/T_c]^{-\gamma} \quad \text{or} \quad \eta \propto [(\varphi - \varphi_c)/\varphi_c]^{-\gamma}, \quad (1)$$

where  $\varphi_c$  is the critical packing fraction (at  $T_c$ ), and  $\gamma$  is a critical exponent. Packing fraction plays here a decisive role in controlling the atomic dynamics of the liquid.

In monoatomic HS systems, packing fraction is the only order parameter that determines dynamic behavior, whereas for the complex real systems, additional effects like size disparity and mixing ratio of particles need to be considered as well [6]. However, in spite of the multiple mixing effects for bi- or multicomponent liquids, a qualitative correlation between slow dynamics and high packing fraction is nevertheless observed for a number of MGF liquids [4,7–11]. The concentration dependence of the atomic dynamics in the melt correlates with the change of its packing fraction as a function of composition in Al-Ni [7], Zr-Ni [8], and Zr-Cu [9] alloys, even in multicomponent Pd- and Zr-based MG systems [10,11]. In most of these cases, the liquid packing fraction was derived by assuming a homogeneous HS-like packing with covalent radii [1]. However, some of these melts are known to exhibit pronounced chemical short-range order (CSRO) at atomic scale [8,12], which leads to the fact that the atomic dynamics of MGF melts cannot be simply explained by the average packing fraction without considering the local structure. For example, a strong correlation of self-diffusion coefficients and CSRO was reported in Al-Ni and Zr<sub>64</sub>Ni<sub>36</sub> systems [13,14]. Hence, these raise an important question whether the average HS packing fraction is a suitable parameter for predicting the

liquid dynamics, especially for metallic glass (MG) formers, in which strong interactions between the constituents cannot be neglected.

An important feature of Al in MGs is its strong chemical interaction with the transition metal (TM) atoms, particularly, late transition metals (LTM) like Cu, Co, and Ni [15–17]. This correlates with the drastic change in the compression plasticity as function of Al content [16], or of fracture toughness when substituted with different LTM atoms [17,18], via tuning of the electronic structure as observed in Zr-LTM-Al systems. However, whether and how such chemical interactions affect the properties of MGF liquids is still an open question. Therefore, we present in the following systematic studies on the liquid dynamics of ternary liquid Zr-(Co, Ni)-Al systems, aiming to find which effect Al has on atomic transport behavior and its correlation with the alloy properties. Both a slow-down of the microscopic transport and of the macroscopic flow behavior upon alloying with Al, manifested by a decrease of the LTM (Co, Ni) self-diffusion coefficient and an increase of the melt viscosity, were observed. In contrast, the average packing fraction of the melt decreases upon Al addition. Thus, the apparent relation between liquid dynamics and average packing density break down in Zr-LTM-Al melts, which is quite different from many other previously studied MGF liquids [4,7–11]. This indicates chemical interactions, found in the corresponding glasses of these alloys in the form of hybrid bonding [16,17], also need to be taken into account to describe liquid dynamics.

Zr<sub>66.7</sub>Co<sub>33.3</sub>, Zr<sub>56</sub>Co<sub>28</sub>Al<sub>16</sub>, Zr<sub>56</sub>Ni<sub>28</sub>Al<sub>16</sub>, and Zr<sub>60</sub>Ni<sub>25</sub>Al<sub>15</sub> samples were prepared by arc melting of Zr (99.97%, smart-elements), Co (99.998%, Alfa Aesar), Ni (99.995%, Alfa Aesar), and Al (99.9999%, Hydro Aluminum) under a Ti-getter high purity Argon (99.9999%) atmosphere. The viscosity and density of the Zr-(Co, Ni)-Al melts are accurately measured over a large temperature range from several hundred degrees above the liquidus temperature down to the deeply undercooled liquid state. Experiments were performed using electrostatic levitation (ESL) in combination with high-speed video diagnostic techniques [19]. The oscillating drop method was used to obtain the viscosity of the samples. The density was determined by employing an image digitizing technique and numerical calculation method on the projected image of the levitated spherical sample. The  $T_L$  of the investigated

\*Corresponding author: [chenchen.yuan@dlr.de](mailto:chenchen.yuan@dlr.de)

binary  $\text{Zr}_{66.7}\text{Co}_{33.3}$ , as well as the ternary  $\text{Zr}_{56}\text{Co}_{28}\text{Al}_{16}$  and  $\text{Zr}_{56}\text{Ni}_{28}\text{Al}_{16}$  are 1323 K, 1253 K, and 1212 K, respectively. These values were measured by differential scanning calorimetry (DSC) at a heating rate of  $20 \text{ K min}^{-1}$ . In the levitation experiments, the temperature was measured by using single-color pyrometry and calibrated according to the  $T_L$ s tested in DSC. The uncertainty is estimated to be about  $\pm 10 \text{ K}$ . Furthermore, the temperature gradient between the surface and the center of the sample is expected to be less than 5 K for the present sample size [20].

The Co self-diffusion in molten  $\text{Zr}_{56}\text{Co}_{28}\text{Al}_{16}$  liquids was investigated by quasielastic neutron scattering (QENS). The experiment was performed on the time-of-flight spectrometer TOFTOF at the research reactor FRM II in Munich [21]. Since Zr-based liquids are chemically highly reactive, they were containerlessly processed using electromagnetic levitation (EML) [22]. Measurements were carried out at temperatures of 1297 K, 1365 K, 1535 K, and 1634 K. An incident neutron wavelength of  $7.0 \text{ \AA}$  was chosen, giving an instrumental energy resolution of  $\delta E \approx 70 \mu\text{eV}$  [full width at half maximum (FWHM)] and an accessible wavenumber range of  $q = 0.4 - 1.6 \text{ \AA}^{-1}$ . The scattering law  $S(q, \omega)$  was obtained by normalizing the raw scattering data to a vanadium standard and correcting for container scattering, also taking into account self-absorption effects. The intermediate scattering function  $S(q, t)$  was obtained by a Fourier transformation of  $S(q, \omega)$  for neutron energy gain. The instrumental energy resolution is removed by a simple division of  $S(q, t)$  with the Fourier transformation of the instrumental resolution function [20,23]. At small momentum transfers  $q$ , the neutron scattering is dominated by incoherent scattering contribution, providing access to the self-correlation function. In Zr-Co-Al melts, cobalt exhibits a dominant incoherent neutron scattering cross section of 4.8 barn, compared with only 0.02 barn for Zr and 0.0082 barn for Al, respectively. This allows us to extract the Co self-diffusion coefficients:  $D_{\text{Co}} = \lim_{q \rightarrow 0} (\tau_q q^2)^{-1}$  [11], where  $\tau_q$  exhibits a characteristic  $q^{-2}$  dependence for  $q < 1 \text{ \AA}^{-1}$ .

Figure 1 shows the temperature-dependent melt viscosity of the ternary  $\text{Zr}_{56}\text{Co}_{28}\text{Al}_{16}$ ,  $\text{Zr}_{56}\text{Ni}_{28}\text{Al}_{16}$ ,  $\text{Zr}_{60}\text{Ni}_{25}\text{Al}_{15}$ , and the binary  $\text{Zr}_{66.7}\text{Co}_{33.3}$  systems. They are compared with the viscosity of  $\text{Zr}_{64}\text{Ni}_{36}$  [19] and that of the multicomponent  $\text{Zr}_{46.75}\text{Ti}_{8.25}\text{Cu}_{7.5}\text{Ni}_{10}\text{Be}_{27.5}$  alloy (Vit4) [24]. Generally, the melt viscosity decreases with increasing temperature. Replacing Co by Ni results in only a minor change of the melt viscosity for both the binary and ternary alloys. In contrast, the addition of Al obviously leads to an increase of the viscosity by more than a factor of three at the respective liquidus temperatures. This disparity increases with decreasing temperature.

A fit using Eq. (1) can well describe the viscosity of the Zr-(Co, Ni)-Al systems, as shown in Fig. 1. A small variation in  $\gamma$  without any systematic trend is observed. For  $T_c$ , where according to MCT liquid dynamics supposedly freezes in, the values obtained for ternary systems are systematically higher compared to those of the binary alloys. The results are listed in Table I.

Interestingly, compared to the Al-containing ternary alloys, the liquid viscosity of one of best MGF systems, Vit4, is

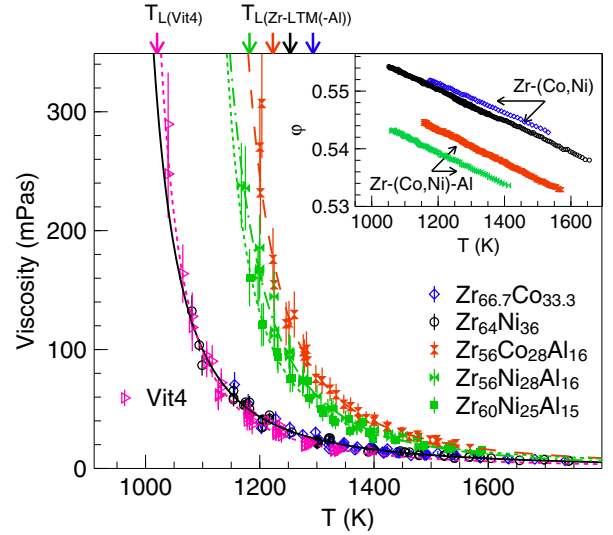


FIG. 1. (Color online) Liquid viscosity of the binary Zr-(Co,Ni) and the ternary Zr-(Co,Ni)-Al alloys. The data for  $\text{Zr}_{64}\text{Ni}_{36}$  and Vit4 are taken for comparison from the work of Brillo *et al.* [19] and Yang *et al.* [24], respectively. The dashed lines and the solid line represent MCT fits for different compositions. The arrows with different color show the liquidus temperature of each composition. The inset shows the corresponding packing fractions, derived from the measured macroscopic liquid densities. The packing fraction of  $\text{Zr}_{60}\text{Ni}_{25}\text{Al}_{15}$  is very close to that of  $\text{Zr}_{56}\text{Ni}_{28}\text{Al}_{16}$  (not shown).

as low as that for the Zr-(Co, Ni) binary systems at similar temperatures. It seems that other alloying elements, such as Ti, Cu, and Be, have a different impact on the viscosity of these Zr-based MGF liquids.

The higher liquid viscosity only indicates an overall slower dynamics in the liquid on the macroscopic level. On the microscopic level, however, not all constituents necessarily contribute equally to the slow dynamics. For example, MD simulations of liquid  $\text{Zr}_{60}\text{Ni}_{25}\text{Al}_{15}$  show a slight tendency for the formation of Al-Al clusters resulting from the competition of the mixing behavior of the Zr-LTM and Zr-Al binaries [25], which leads to a different Al dynamics compared with the other components in the melt. QENS provides here a unique

TABLE I. The liquidus temperatures  $T_L$ ,  $\gamma$ ,  $T_c$  from a fit according to MCT scaling law on the liquid viscosity, and the packing fraction  $\phi_c$  at  $T_c$ , of the binary Zr-(Co,Ni), ternary Zr-(Co,Ni)-Al, and the multicomponent Vit4 liquids. The determined  $T_c$ s show large uncertainties since the viscosities obtained are still well above the  $T_c$ s. Hence, the  $T_c$ s here are not necessarily comparable to those obtained from other data. However, the ternary alloys exhibit systematically higher  $T_c$  than the binary alloys.

Composition	$T_L$ (K)	$\gamma$	$T_c$ (K)	$\phi_c$
$\text{Zr}_{66.7}\text{Co}_{33.3}$	1323	1.818	$892 \pm 18$	0.559
$\text{Zr}_{64}\text{Ni}_{36}$	1283	1.818	$927 \pm 22$	0.558
$\text{Zr}_{56}\text{Co}_{28}\text{Al}_{16}$	1253	1.860	$1081 \pm 12$	0.547
$\text{Zr}_{56}\text{Ni}_{28}\text{Al}_{16}$	1212	2.266	$1015 \pm 30$	0.545
$\text{Zr}_{60}\text{Ni}_{25}\text{Al}_{15}$	1213	1.571	$1076 \pm 25$	0.545
Vit4	1050	1.903	$952 \pm 14$	0.514

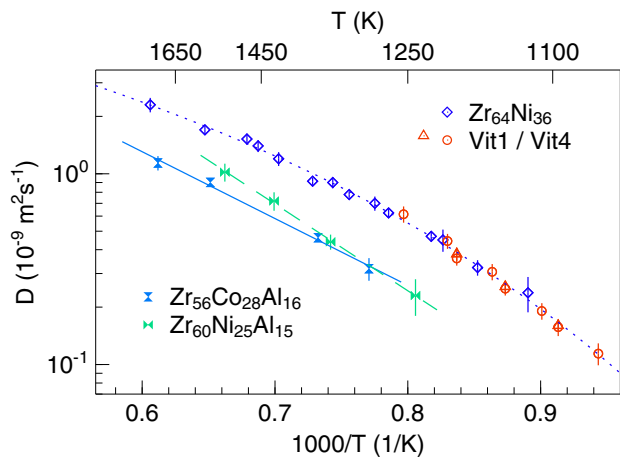


FIG. 2. (Color online) Temperature-dependent self-diffusion coefficients of Co in liquid  $\text{Zr}_{56}\text{Co}_{28}\text{Al}_{16}$  and of Ni in a corresponding  $\text{Zr}_{60}\text{Ni}_{25}\text{Al}_{15}$  as well as in the binary  $\text{Zr}_{64}\text{Ni}_{36}$  melt [8,26]. The Ni self-diffusion coefficients for Vit1 and Vit4 are also included for comparison [11,24].

possibility to investigate the microscopic atomic dynamics and how individual constituents in the melt contribute to the sluggish liquid dynamics.

Figure 2 shows the measured self-diffusion coefficient  $D$  of Co in molten  $\text{Zr}_{56}\text{Co}_{28}\text{Al}_{16}$ . The Ni self-diffusion coefficients of  $\text{Zr}_{64}\text{Ni}_{36}$  [8],  $\text{Zr}_{60}\text{Ni}_{25}\text{Al}_{15}$  [26], and Vit1&4 [11,24] are plotted for comparison. In  $\text{Zr}_{56}\text{Co}_{28}\text{Al}_{16}$  an Arrhenius-type behavior  $D_{\text{Co}} = D_0 \exp(-E_A/k_B T)$  is observed in the investigated temperature range with an activation energy  $E_A = 0.70 \pm 0.02$  eV. The Co self-diffusion coefficients in  $\text{Zr}_{56}\text{Co}_{28}\text{Al}_{16}$  are quite close to the Ni self-diffusion coefficients in the corresponding  $\text{Zr}_{60}\text{Ni}_{25}\text{Al}_{15}$  melt. However, both are about a factor of two lower than those in the corresponding binary or other multicomponent Zr-based systems at the same temperature. Thus, similar to the observation of the melt viscosity, the addition of Al also slows down the diffusion of LTM atoms in Zr-(Co,Ni)-Al systems compared with the corresponding binary melts, whereas substituting Co by Ni results only in a comparatively minor change of the diffusion coefficient.

Whereas for  $\text{Zr}_{56}\text{Co}_{28}\text{Al}_{16}$  at small  $q$  values the incoherent scattering contribution of LTM-atoms dominates the total scattering intensity, for  $q > 1 \text{ \AA}^{-1}$  coherent scattering contributions become increasingly important. The total coherent scattering contribution is a weighted sum of the constituent pair correlation functions. In  $\text{Zr}_{56}\text{Co}_{28}\text{Al}_{16}$  the Zr-Zr pair correlation contributes more than 70% to the total coherent scattering intensity followed by Zr-Co and Zr-Al of about 13% and 10%, respectively. Thus, the  $q$ -dependent intermediate scattering function  $S(q,t)$  allows for a direct comparison between the Co self dynamics and the collective Zr-Zr, Zr-Co, and Zr-Al dynamics. These collective relaxation processes are also considered to underlie the viscous behavior of the melt on the macroscopic scale [27].

Figure 3(a) shows the rescaled intermediate scattering function  $S(q,t/\tau_q)/f_q$  according to their corresponding structural relaxation times  $\tau_q$  and amplitudes  $f_q$ . It can be seen that, despite the variation of the structural relaxation time and length

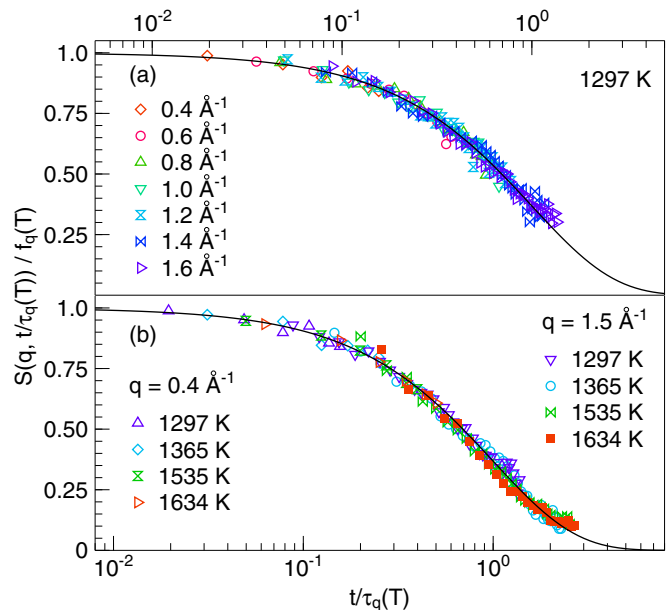


FIG. 3. (Color online) (a) Time- $q$  superposition  $S(q,t/\tau_q)/f_q$  of the density correlation function obtained by rescaling it with  $f_q$  and  $\tau_q$  at each respective  $q$  value. (b) Time-temperature superposition master curve  $S[q,\tau_q(T)]/f_q(T)$  at  $q = 0.4 \text{ \AA}^{-1}$  and  $q = 1.5 \text{ \AA}^{-1}$ , respectively, rescaled with the relaxation time  $\tau_q(T)$  amplitude  $f_q(T)$  at respective temperatures. The solid line represents in both cases a simple exponential function.

scales, and the different incoherent and coherent contributions to  $S(q,t)$  at different  $q$ , the rescaled intermediate scattering functions fall onto a single master curve. Also, a time-temperature superposition can be obtained for both small and large momentum transfers, as shown in Fig. 3(b). No change of the line shape of the measured intermediate scattering function is observed in the accessible  $q$  and temperature range. In both cases the master curve can be described by a simple exponential decay. No stretching behavior can be resolved at these relatively high temperatures. Thus, we conclude that the separation of relaxation timescales between these different correlation functions is small over the entire experimental  $q$  and temperature window. Apparently, the addition of 16 at% Al slows down the atomic dynamics of all components.

According to the prediction of MCT, the packing fraction is an important control parameter for the atomic dynamics in dense liquids. Hereby, we further derived the effective HS packing fraction  $\varphi$  from the measured liquid density by

$$\varphi = \frac{1}{6} \pi n \bar{d}^3, \quad (2)$$

where  $\frac{1}{6} \pi \bar{d}^3$  is the mean HS volume according to the covalent atomic radii [28].  $n$  is the number density of atoms per unit volume, calculated from the density of a liquid as  $n = \rho N_A / \bar{M}$ , where  $N_A$  is the Avogadro constant and  $\bar{M}$  is the average molar mass of the alloy. The inset in Fig. 1 shows the resulting  $\varphi$ . The density data of  $\text{Zr}_{64}\text{Ni}_{36}$  was taken from Ref [19]. It can be seen that  $\varphi$  decreases upon alloying of Al to the binary Zr-LTM systems, and an addition of 16 at% of Al leads to a reduction of the liquid packing fraction by about

1.5%. This is not expected from observations on other melt from the MCT prediction, where a slower liquid dynamics is usually associated with a higher packing fraction [5].

Previous electronic structure studies on Zr-(Cu,Co,Ni)-Al MG give convincing experimental evidence for the *sp-d* hybridization between Al and transition metal, where the formation of strong chemical bonding is expected [16,29,30]. The observation of Co  $L_{23}$  edges, and the prepeaks near Al  $L_{23}$  and K edges in the electron-energy-loss spectroscopy [17] of  $Zr_{56}Co_{28}Al_{16}$  MG indicate a combination of angular momentum coupling and partial occupation of *d* orbitals, which is a clear evidence for covalent-like Al-TM *p-d* (or Zr-Co *d-d*) bond formation. For Al-TM systems exhibiting a pronounced CSRO, e.g., Al-Co, *ab initio* calculations on the density of state (DOS) show a pseudogap at the top of the *d*-band close to the Fermi level [30], which is again the signature of *sp-d* hybridization. Such pseudogap on the *d* state was further confirmed by the evolution of  $^{27}Al$  isotropic shifts in NMR study [16,17] of Zr-LTM (Cu, Ni, or Co)-Al ternary glass system. Thus, for these MGs, Al tends to form bonding of a more covalent nature with TMs.

Recent diffraction and MD simulation studies on Zr-Cu-Al glasses show a strong bonding between Al with the Cu atoms. A shorter interatomic distance between the Cu and Al atoms has been observed [15]. This has also been found in other alloy systems, where a strong chemical interaction is expected to reduce the effective interatomic distance compared with a simple weighted sum of the atomic radii [15,31,32]. It should be noted that, if this also holds for Zr-(Co,Ni)-Al, taking a smaller atomic radius (from the interatomic distance) would result in an even lower packing fraction, although obviously locally the atoms are more densely packed. On the other hand, in the simulation by Cheng *et al.* [15], the degree of connectivity of short-range ordered clusters increases upon Al addition. Both a strong bonding and the increasing connectivity of clusters leads to a slowing down of the atomic dynamics. Thus, the average HS packing fraction is not a suitable parameter for predicting the liquid dynamics in those systems.

This is consistent with our experimental observations. We propose that chemical interactions between Al and LTM atoms, similar to the form of a hybridization bonding involving in corresponding glasses [17], remain even in the equilibrium liquid and impede atomic motion. We note that MCT is able to capture such chemical features, provided that the partial structure factors are available [14]. However, experimental assessment of partial structure factors of ternary alloys is difficult. In this case computer simulations can be very helpful to further understand the mechanism [33].

It is also interesting to note that comparing the liquid viscosity of a number of other Zr-based MGF liquids, it seems that Al containing melt [Zr-(Co,Ni)-Al, Vit105, Vit106, Vit106a] exhibit generally higher viscosity than the non-Al containing melts [Zr-(Co,Ni), Vit101, Vit4] [34]. Furthermore, when the temperature was scaled with the respective liquidus temperature, the studied Zr-(Co, Ni)-Al melts give a tendency: the better glass former with additional Al has the slower dynamics. This shows that, liquid kinetics is also one of important factors that needs to be considered to understand the effect of Al on the GFA [35]. In conclusion, a sluggish transport behavior has been observed in Zr-(Co,Ni)-Al melts. The addition of Al leads to a slowing down of the liquid dynamics of all components. In contrast, the packing fraction derived assuming a HS mixture of the ternary alloys decreases compared to that of the corresponding binary melts. This shows that in these Al-bearing melts, chemical interactions play an important role in determining the liquid dynamics, which come along with an improved GFA.

We thank J. Gegner and P. Heintzmann for their support during the experiment at FRM II and W. H. Wang, Th. Voigtmann, and Z. Evenson for the critical discussion and modification of the manuscript. C.C.Y. is supported by the German Academic Exchange Service through the DLR-DAAD programme (Grant No. 96). The financial support provided by the Deutsche Forschungsgemeinschaft (DFG) under Grant No. ME1958/10-1 is gratefully acknowledged.

- 
- [1] U. Balucani and M. Zoppi, *Dynamics of the Liquid State* (Clarendon, Oxford, 1994).
- [2] K. Ohsaka, S. K. Chung, W. K. Rhim, A. Peker, D. Scruggs, and W. L. Johnson, *Appl. Phys. Lett.* **70**, 726 (1997).
- [3] I.-R. Lu, G. Görler, H. Fecht, and R. Willnecker, *J. Non-Crystal. Solids* **312–314**, 547 (2002).
- [4] S. M. Chathoth, B. Damaschke, M. M. Koza, and K. Samwer, *Phys. Rev. Lett.* **101**, 037801 (2008).
- [5] W. Götze, in *Liquids, Freezing and Glass Transition, Les Houches 1989, Session LI*, edited by J. Hansen, D. Levesque, and J. Zinn-Justin (North-Holland, Amsterdam, 1991).
- [6] G. Foffi, W. Götze, F. Sciortino, P. Tartaglia, and T. Voigtmann, *Phys. Rev. Lett.* **91**, 085701 (2003).
- [7] S. Stüber, D. Holland-Moritz, T. Unruh, and A. Meyer, *Phys. Rev. B* **81**, 024204 (2010).
- [8] D. Holland-Moritz, S. Stüber, H. Hartmann, T. Unruh, T. Hansen, and A. Meyer, *Phys. Rev. B* **79**, 064204 (2009).
- [9] F. Yang, D. Holland-Moritz, J. Gegner, P. Heintzmann, F. Kargl, C. C. Yuan, G. G. Simeoni, and A. Meyer, *Europhys. Lett.* **107**, 46001 (2014).
- [10] S. M. Chathoth, A. Meyer, H. Schober, and F. Juranyi, *Appl. Phys. Lett.* **85**, 4881 (2004).
- [11] A. Meyer, W. Petry, M. Koza, and M.-P. Macht, *Appl. Phys. Lett.* **83**, 3894 (2003).
- [12] V. Wessels *et al.*, *Phys. Rev. B* **83**, 094116 (2011).
- [13] S. K. Das, J. Horbach, M. M. Koza, S. M. Chathoth, and A. Meyer, *Appl. Phys. Lett.* **86**, 011918 (2005).
- [14] T. Voigtmann, A. Meyer, D. Holland-Moritz, S. Stüber, T. Hansen, and T. Unruh, *Europhys. Lett.* **82**, 66001 (2008).
- [15] Y. Q. Cheng, E. Ma, and H. W. Sheng, *Phys. Rev. Lett.* **102**, 245501 (2009).
- [16] X. K. Xi, M. T. Sandor, H. J. Wang, J. Q. Wang, W. H. Wang, and Y. Wu, *J. Phys.: Condens. Matter* **23**, 115501 (2011).
- [17] C. C. Yuan, X. Shen, J. Cui, L. Gu, R. C. Yu, and X. K. Xi, *Appl. Phys. Lett.* **101**, 021902 (2012).
- [18] Q. He, Y.-Q. Cheng, E. Ma, and J. Xu, *Acta Mater.* **59**, 202 (2011).
- [19] J. Brillo, A. I. Pommrich, and A. Meyer, *Phys. Rev. Lett.* **107**, 165902 (2011).

- [20] T. Kordel, D. Holland-Moritz, F. Yang, J. Peters, T. Unruh, T. Hansen, and A. Meyer, *Phys. Rev. B* **83**, 104205 (2011).
- [21] T. Unruh, J. Neuhaus, and W. Petry, *Nucl. Instr. Meth. A* **580**, 1414 (2007).
- [22] J. Brillo and I. Egry, *Int. J. Thermophys.* **24**, 1155 (2003).
- [23] A. Meyer, S. Stüber, D. Holland-Moritz, O. Heinen, and T. Unruh, *Phys. Rev. B* **77**, 092201 (2008).
- [24] F. Yang, T. Unruh, and A. Meyer, *Europhys. Lett.* **107**, 26001 (2014).
- [25] M. Guerdane and H. Teichler, *Phys. Rev. B* **65**, 014203 (2001).
- [26] D. Holland-Moritz, S. Stüber, H. Hartmann, T. Unruh, and A. Meyer, *J. Phys.: Conf. Ser.* **144**, 012119 (2009).
- [27] J. P. Hansen and I. R. McDonald, *Theory of Simple Liquids* (Academic Press, London, 1986).
- [28] L. Pauling, *J. Am. Chem. Soc.* **69**, 542 (1947).
- [29] C. C. Yuan, J. F. Xiang, X. K. Xi, and W. H. Wang, *Phys. Rev. Lett.* **107**, 236403 (2011).
- [30] D. Mayou, D. Nguyen-Manh, A. Pasturel, and F. Cyrot-Lackmann, *Phys. Rev. B* **33**, 3384 (1986).
- [31] I. Kaban, P. Jónvári, V. Kokotin, O. Shuleshova, B. Beuneu, K. Saksl, N. Mattern, J. Eckert, and A. L. Greer, *Acta Mater.* **61**, 2509 (2013).
- [32] A. Yakymovych, I. Shtablayvi, and S. Mudry, *J. Alloys Comp.* **610**, 438 (2014).
- [33] P. Kuhn, J. Horbach, F. Kargl, A. Meyer, and T. Voigtmann, *Phys. Rev. B* **90**, 024309 (2014).
- [34] Z. Evenson, T. Schmitt, M. Nicola, I. Gallino, and R. Busch, *Acta Mater.* **60**, 4712 (2012).
- [35] W. H. Wang, *Progr. Mater. Sci.* **52**, 540 (2007).